The effects of transient flow conditions on the aerodynamics of an LCV concept using CFD and wind tunnel experiments

A Kremheller [1], M Moore [1], G Le Good [2], D Sims-Williams [3], J Newbon [3], R Lewis [4]
[1] Nissan Motor UK, UK
[2] G L Aerodynamics Ltd, UK
[3] Durham University, UK
[4] TotalSim Ltd, UK

ABSTRACT

This paper aims to illustrate the differences of aerodynamic coefficients under conventional steady state conditions and a variety of turbulent conditions. Two 30% scale models were tested in the Durham University Scale model wind tunnel that offers the capability of testing with a turbulence generation system (TGS). Turbulence length scales are in the range of 1m to 17m based on model scale and turbulence intensities in the range of 2.5% to 10%. It was found that, while non-zero yaw conditions can generally be expected to increase drag, the drag increments under unsteady flow conditions were less than would be predicted by a quasi-steady analysis. Steady and unsteady environments showed similar differences in the drag of different vehicles, but the effects of more detailed configuration changes were found to depend on the test environment.

1 INTRODUCTION

Conventional CFD simulations and wind tunnel tests are used to develop and improve the aerodynamic performance of vehicles. These development tools are constantly optimised to improve correlation and efficiency in order to not only deliver lower drag coefficients, but also to predict the final absolute results accurately at an early stage of the development phase (1). In addition, the determination of fuel consumption and CO_2 emissions under on-road conditions is of increasing interest to the customer. As aerodynamic drag is a major contributor to fuel economy at high driving speeds the aerodynamicist must investigate real world conditions and expand the conventional development envelope. Aerodynamic targets for vehicle development programmes are usually set utilizing wind tunnel configurations in steady state onset flow, with low turbulence levels (< 1%) and at 0 degree yaw. This is mainly because this condition is relatively easy to specify and replicate in different wind tunnels, making it easier to standardise test conditions. However, the environment on-road is significantly different to the steady onset flow condition as described above. It is influenced by temporal and spatial variations of the natural wind which leads to variations in onset velocity and direction experienced by the vehicle. Depending on the topographical surroundings, the wind environment and unsteady turbulence effects can vary substantially, and can impact the aerodynamic properties of the customer's vehicle. In contrast to steady state conditions, a description of the on-road conditions is complex and hence no requirement or regulations for the unsteady environment exist to this date.

Numerous research programmes have been conducted in recent years to characterise the unsteady real-world environment and to investigate the effects of this environment. This work has included CFD simulations, on-road experiments and the use of wind tunnels with turbulence generation systems.

The aerodynamic drag increase with variation of yaw angle were investigated by Howell (2), (3) and Windsor (4). Both concluded that the yaw sensitivity can vary considerably between vehicle types and that the conventional zero degree yaw onset flow used for aerodynamics development in wind tunnels is not representative of real-world conditions.

Effects of upstream turbulent boundary conditions in CFD simulations were explored by Gaylard (5) and found that the drag reduction effectiveness of aero parts, such as front and rear tyre deflectors, was reduced when upstream turbulence was added. D' Hooge (6) investigated the aerodynamic yaw response by means of time varying cross-flow as well as upstream turbulence in CFD simulations. Upstream turbulence resulted in an increase of overall drag values.

Extensive research has been carried out by Wordley and Saunders (7) into the determination of turbulent intensities, turbulent length scales and how these are influenced by terrain, road side obstacles and vehicles.

Additionally, Sims-Williams (8) highlighted which length scales have the most significant impact on vehicle stability and comfort. A key point made in this research is that these cannot be simulated or evaluated using steady state methods.

Scale model wind tunnels have recently been modified to offer the capability of turbulence generation systems (TGS). Mankowski (9) described the update of the Durham scale model wind tunnel and concluded that an environment similar to that found on road can be simulated with the TGS. Work done by Stoll (10) at the IVK Model Scale Wind Tunnel reported that time-averaged aerodynamic drag on a DrivAer model is increased under unsteady conditions. Additionally, configuration changes might not lead to the same results and can have contrary behaviour in steady and unsteady conditions.

This paper aims to illustrate the differences of aerodynamic coefficients under conventional steady state conditions and a variety of unsteady conditions. The most important variation in onset flow on road is related to lateral velocities and hence unsteady conditions are distinguished in the yaw time trace and yaw probability distribution. Turbulence length scales are in the range of 1m to 17m and turbulence intensities in the range of 2.5% to 10%. Two 30% scale models were tested in the Durham University 2m wind tunnel using the turbulence generation system (TGS) available in this facility.

The two models represent stages of a vehicle development program; the baseline at the start of the development and the final optimised shape. For the design development from baseline to the final shape, steady-state DES CFD simulations were used to improve the upper-body and under-floor geometry. A description of the effects of the unsteadiness as measured in the scale model tunnel on overall aerodynamic properties and configuration changes by means of add-on parts will be given.

Objectives of the investigation were to answer:

-What impact does an unsteady onset flow have on time-averaged aerodynamic drag compared with test conditions typically used for development?

-What are the challenges of non-dimensionalisation of aerodynamic coefficients in an unsteady test environment?

-In terms of drag and lift, are configurations ranked in the same order based on steady and unsteady onset flow environments? Would the same design decisions be made if the target environment were unsteady rather than steady?

2 LCV CONCEPT DEVELOPMENT

A thorough description of the development of the LCV concept was published by Kremheller (11) and is only summarised in this paper. As a pre-condition, a Nissan NV200 van was used and changed according to a new packaging layout that required a cabin height increase, resulting in an increase in frontal area of 11% with a respective drag increase of 8%. A design optimisation study using steady-state DES CFD simulations was used to improve the upper-body and under-floor in order to recover the increased CdA. A close collaboration between the aerodynamicists and the styling team led to a reduction in CdA by 38% from the updated NV200 with new hard points. The evaluation models were simplified by closing the cooling apertures, applying a flat floor and removing the door mirrors. Results from the CFD simulations are shown in figure 1.

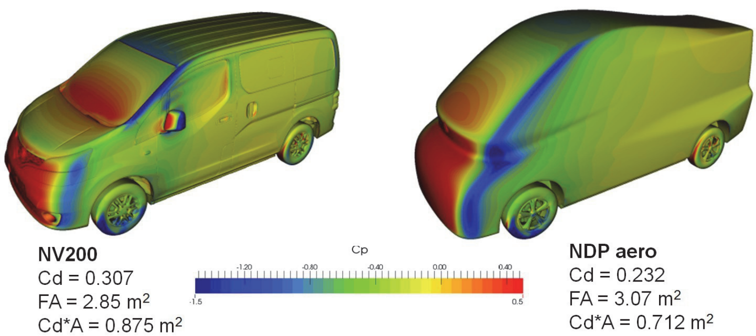

Figure 1. Results and c_p distribution from steady-state DES CFD simulations; NV200 (left) and NDP (right).

3 METHODOLOGY

3.1 Scale Model

The design of the model featured two interchangeable-shell upper bodies CNC-machined in lightweight foam – one each for the NV200 and NDP Aero styles. The bodies were in turn attached to a common support structure which consisted of an aluminium armature, aluminium wheel support brackets and aluminium wheel studs, together with a smooth under floor and non-rotating wheels machined in lightweight foam. For compatibility with the dimensions of the Durham University wind tunnel a scale of 30% was chosen. The two models installed in the wind tunnel are shown in figure 2, showing the NDP Aero and NV200 models from upstream and downstream viewpoints respectively.

In addition, 64 pressure tapings were installed in each upper body shell on roof, body side, front and rear to record time resolved pressure data during the wind tunnel tests.

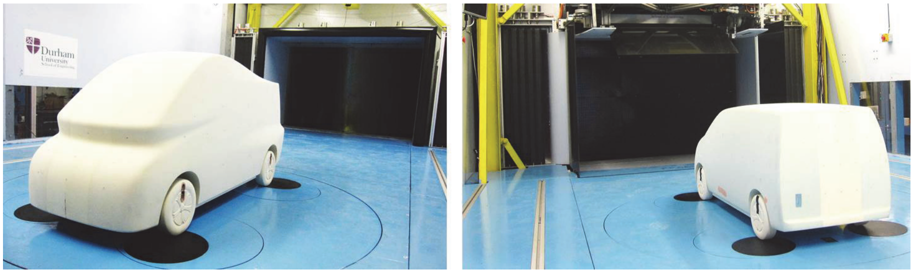

Figure 2. 30% scale models of the NDP (left) and NV200 (right) installed in the Durham Scale Wind tunnel.

3.2 Wind Tunnel

Wind tunnel tests were conducted in the Durham University 2m Wind Tunnel. This is a ¾ open jet tunnel with a jet area of $2m^2$ and aspect ratio of 3:2. For this project the tunnel was operated in fixed ground mode with the model mounted to the under floor balance. The tunnel design and balance are described by Sims-Williams and Dominy (12), (13). The mechanical natural frequencies of the balance with the model installed were measured via an impulse test and the first natural frequency was 13 Hz. Time resolved force balance measurements were therefore low pass filtered using a 10th order Butterworth filter at 10 Hz.

The tunnel has been equipped with an active system for generating programmable, time-varying onset flow conditions, referred to as a "Turbulence Generation System" (TGS). It should be emphasised that the unsteady flows generated are large scale (i.e.: length scales on the scale of the vehicle) as would be experienced by a vehicle driving on the road, including on a moderately windy day. These unsteady flows are several orders of magnitude larger in physical scale than typical turbulence experienced in a wind tunnel. Hence the system could be described as producing dynamic yaw rather than "turbulence". The design and commissioning of the TGS in the Durham tunnel is described by Mankowski et al (9). Time resolved data recording was synchronised to the motion of the TGS. Surface pressures were measured using an ESP Pressure Scanner.

Time-resolved measurements were made using a 5-hole probe on the wind tunnel overhead traverse. Measurements were made for the empty test section and with the probe positioned over the roof of the model as shown in figure 3. The latter were made simultaneously with the balance measurements. This location is equivalent to a location that would be used for on-road measurements on a vehicle (eg: as per Oettle et al (14) or Mankowski et al (9)). The pneumatic transfer function for the tubes connecting the probe to the remote transducers was measured and transfer function correction applied as per (15).

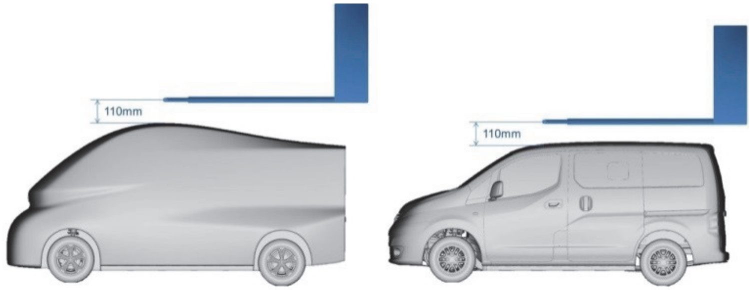

Figure 3. Schematic of the probe location on NDP and NV200.

4 RESULTS

The main objective of this study was to compare results obtained from conventional steady force measurements with those obtained from time varying measurements. The unsteady modes used are presented, issues of non-dimensionalisation are discussed, the effects of different unsteady simulation modes in comparison to steady results for both scale models are analysed as well as the effects of small configuration changes on the NDP model.

4.1 Steady state results

Conventional steady force measurements are non-dimensionalised using the tunnel velocity obtained using the nozzle method and then blockage corrected based on SAE SP-1465 (16). The blockage corrected aerodynamic drag coefficient for NV200 and NDP model are shown in figure 4. The NV200 drag coefficient is C_{D0} = 0.326 and the NDP drag coefficient is C_{D0} = 0.282.

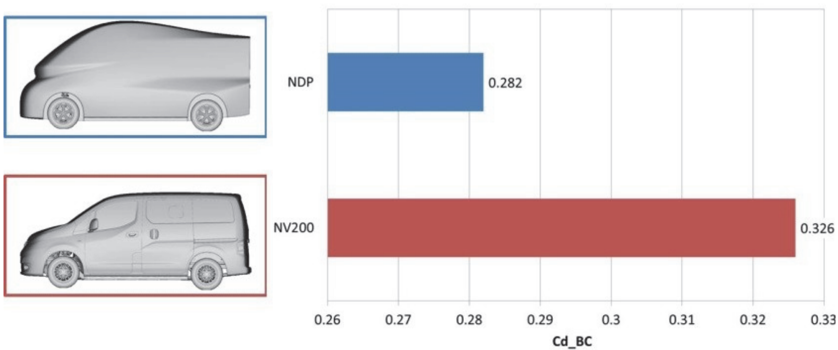

Figure 4. Blockage corrected drag coefficient at 0 yaw angle for NV200 and NDP.

The drag increase with increasing yaw angle for the NV200 and NDP geometries is shown in figure 5. Both vehicles have a defined drag minimum at 0 degree yaw with a lesser tendency for drag increase at yaw for the NDP model. The drag rise and asymmetry as found on both vehicles is typical for MPV's (2),(3).

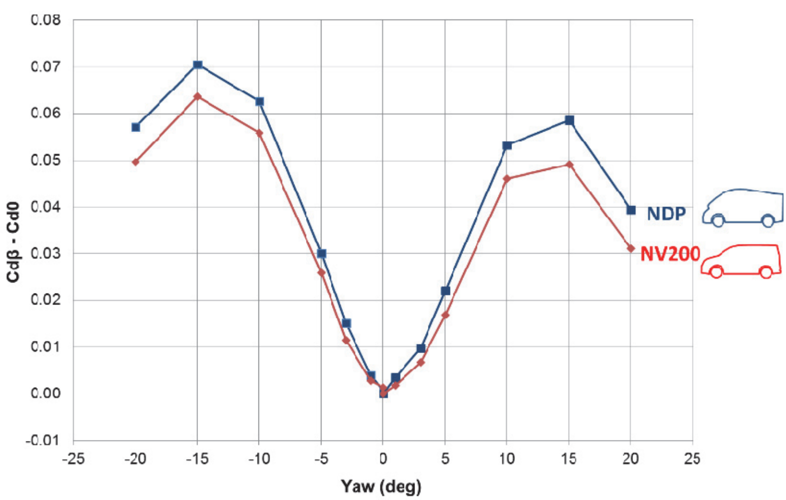

Figure 5. Drag increase with yaw angle for NV200 and NDP.

4.2 Unsteady Modes

The Durham TGS allows for a variety of different turbulence modes. In principle, the TGS is a tool for the generation of dynamic yaw, which is recognised as the most important mode of onset flow unsteadiness for road vehicles (8). Unsteady flows can be characterised by turbulence intensity (TI) and length scale (TLS) or, more completely, by considering the yaw angle probability density distribution and spectrum. Based on previous work (7), three main TGS modes were chosen with characteristic lateral turbulence intensities (TI_y) and turbulence length scales (TLS_y) as listed in table 1.

Table 1: Example of TGS modes used at the Durham Wind Tunnel.

TGS Modes	Measured	
	TIy	TLSy at 30% scale
Harmonic Full Amp 4Hz	10 %	1 m
Inflections	5 %	2 m
Flanders D4.5 0.03Hz	2.5 %	17 m

Harmonic modes are attractive because they can be created by less sophisticated systems and because they provide simple cases for analysis but they have a yaw angle probability density distribution that tends to large yaw angles and is not at all representative of that seen in practise. The "Inflections" mode introduced by Mankowski et al (9) is derived from a real 32 second measured on-road transient, scaled in time for use at model scale. Flanders (17) modes are periodic modes but designed to reproduce realistic on-road yaw angle probability density distributions. Flanders modes have the highest probability near zero yaw, with decreasing probabilities of higher yaw angles. This is in contrast to harmonic modes where the highest probability occurs at or near the peak yaw angle. An overview of the time signal and yaw probability distribution for the TGS modes is shown in figure 6. Additionally, the frequency range of the Harmonic mode was varied from 0.3 Hz to 8 Hz.

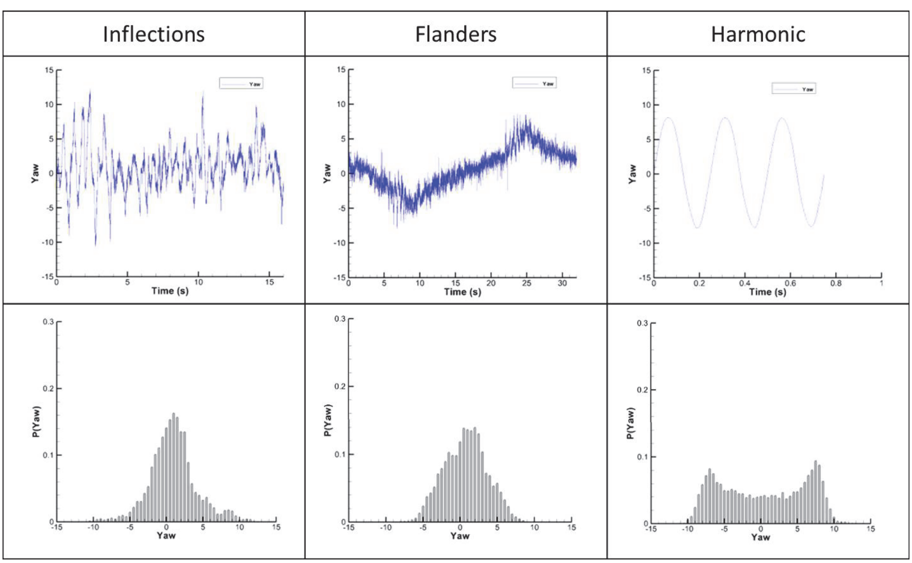

Figure 6. Overview of the yaw time trace and yaw probability distribution for the main TGS modes; Inflections, Flanders and 4Hz Harmonic.

4.3 Definition of drag coefficient

In order to attempt to quantify the impact of onset flow unsteadiness on drag considerable care is needed to make a fair comparison. The most significant effects of a realistic onset flow are likely to be the quasi-steady impacts of the range of yaw angles included and the average onset dynamic pressure.

In ground vehicle tunnel testing the convention is to report vehicle-aligned drag non-dimensionalised using the total tunnel velocity. Of course it should be remembered that with a yawed flow the resultant velocity (ie: tunnel velocity) is not generally equal to the driving velocity. We know that drag will depend strongly on yaw angle and on the square of the resultant onset velocity and so the yaw and resultant velocity content of any time-varying onset flow will play a leading role in the time-averaged drag force experienced. In this work, as is conventional, vehicle-aligned drag is reported non-dimensionalised by the average resultant dynamic pressure.

Wind tunnel interference (linked to blockage and tunnel pressure gradients) is well known to impact measured forces and good correction methods are available to remove this effect (16), (18); but these methods generally focus only on the zero yaw case. In a transient flow the situation becomes more complex because the effective blockage is varying with time. The Durham tunnel operates with a slightly larger nozzle width in TGS mode to maintain the test property comfortably within the jet core; further, the jet width varies dynamically with yaw as part of the unsteady cycle. For this reason no blockage correction is applied with the tunnel in TGS-mode. It should be recognised that an unsteady onset flow brings many complexities, for example transients in resultant velocity at constant stagnation pressure necessarily imply transients in static pressure, and hence moving static pressure gradients.

Figure 7 illustrates the scale of the various effects outlined above for the baseline NV200 geometry, highlighting that it is important to make a fair comparison in order to attempt to quantify impacts of the unsteady aspects of the onset flow on the absolute drag value.

The solid bars in figure 7 represent steady, zero yaw cases. The conventional operation of the tunnel: non-TGS mode, zero yaw with blockage correction following (16) is denoted "Steady-BC" and gives a drag coefficient of 0.326. Without blockage correction ("Steady-RAW") the corresponding drag coefficient would be reported as 0.310 (as an open-jet tunnel with a long test section the measured drag for this model is ~16 counts below the value that would be obtained in an infinite test section). "Steady TGS mode" corresponds to the TGS setup (modified jet dimension and tunnel diffuser geometry) but without the TGS running and results in a lower measured drag by ~13 counts.

The pattern filled bars in figure 7 represent the Inflections mode introduced by Mankowski et al (9). The quasi-steady bar represents the drag calculated using the yaw sensitivity of the steady results combined with the instantaneous yaw angles generated by the TGS unsteady flow field measured in the empty test section for this particular unsteady mode. The resultant velocity varies with yaw and so the combined variation of dynamic pressure and yaw angle is taken to account in the quasi-steady bar. This indicates that a quasi-steady analysis, akin to a wind-averaged drag, would lead to a drag coefficient increase of 19 counts. However, the time average of the unsteady drag measured for the actual unsteady case is within ~1 count of the steady zero yaw TGS-mode measurement.

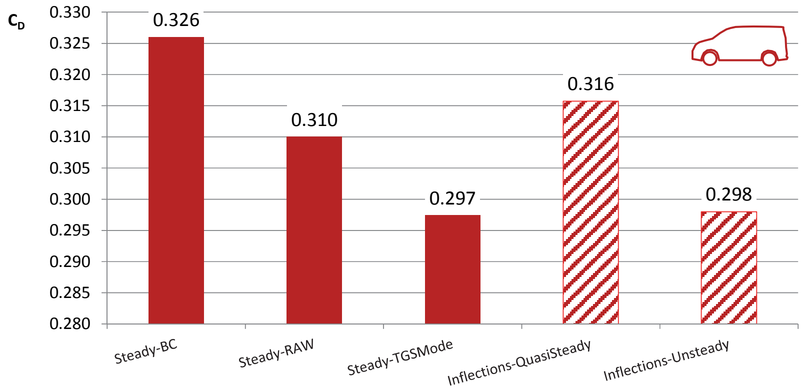

Figure 7. Comparisons of different C_D definitions for the NV200 baseline. In solid bars the steady results and in pattern filled bars the unsteady results using the Inflections mode.

4.4 Impact of Unsteady Onset Flow on Drag

In this section all time averaged results from the unsteady measurements are denoted with TGS and are non-dimensionalised with the probe velocity of the empty test section. The increment in drag coefficient between steady results and unsteady TGS modes for NV200 and NDP are shown in figure 8. Results show that differences for quasi-steady drag increment for the Flanders and Inflections modes are almost the same as both modes have a similar yaw probability distribution. NDP has slightly less sensitivity to yaw (figure 5) and so less drag increment is expected.

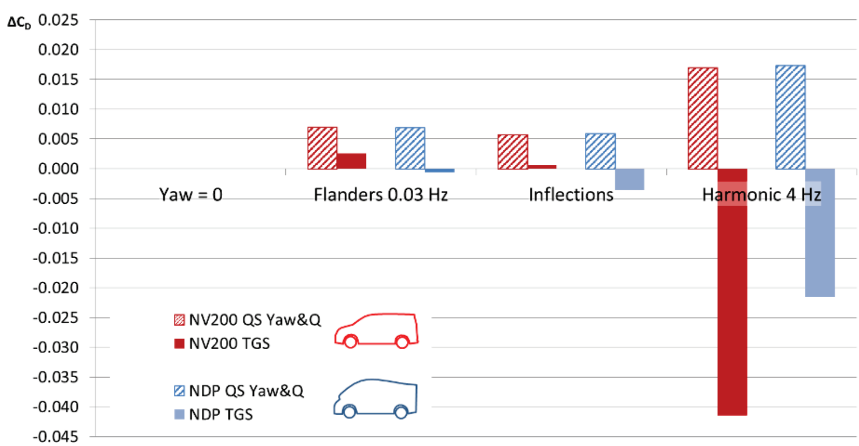

Figure 8. Variation of unsteady C_{d_TGS} and C_{d_QS} to steady results of the NV200 and NDP models. Solid bars represent time averaged unsteady results and hatched bars are quasi-steady expectation for same yaw and dynamic pressure variation.

Again, the drag increment with the actual unsteady flow is less than expected from a quasi-steady analysis and the NDP sees a slight drag reduction for the Inflections mode. In order to understand this, figure 9 illustrates the waistline surface pressure distribution in this case including the delta from the quasi-steady expectation to the time-average of the unsteady result. It can be seen that while pressures around the stagnation pressure average to the quasi-steady expectation, average pressures elsewhere are higher. This higher pressure, on average, acting on the base generates the drag saving, relative to the quasi-steady expectation. It is planned to investigate this mechanism in more detail in the future.

The results for the 4 Hz harmonic mode show a strongly contrasting trend. The time averaged TGS results for NV200 and NDP show a significant drag reduction where a quasi-steady analysis predicts a drag increment. While this is interesting, it should be emphasised that this case is not representative of real on-road conditions.

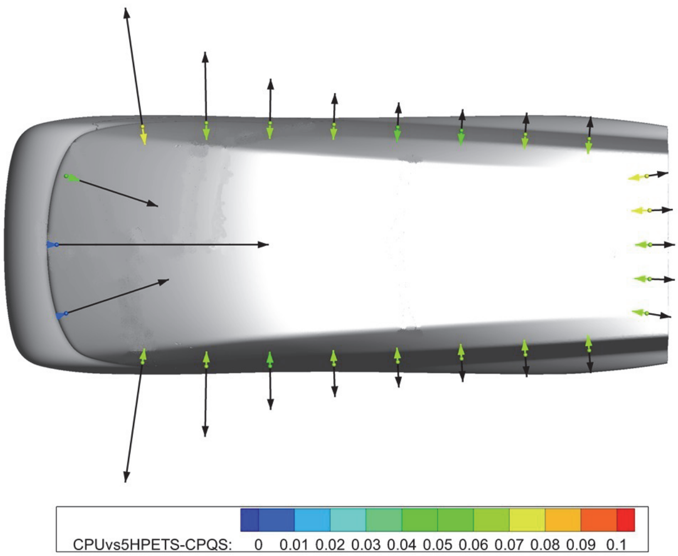

Figure 9. Waistline surface pressure distribution (black) for the Inflections case. Colour vectors represent the delta from the quasi-steady prediction to the time-average of the unsteady measurement.

While the drag level will depend on the onset flow conditions (steady or unsteady) and so can be expected to be different in different environments it should be emphasised that the approach to non-dimensionalisation in a situation where velocity and flow direction vary in time and in space can significantly influence the conclusion drawn. Arguably a better question is whether the relative performance of different designs will be the same in steady and unsteady environments.

The NV200 model can be considered the baseline at the start of an optimisation activity and the NDP model the final optimised configuration. Figure 10 shows the drag saving between the NV200 and NDP for steady and unsteady conditions. The difference in the steady C_D with the tunnel in conventional configuration is 0.044 counts and a quasi-steady analysis expects an almost identical benefit for the range of yaw angles present in any of the unsteady modes considered. The actual unsteady performance benefit is within 2 counts of this for the Flanders and Inflections modes, with a slightly larger impact just from the operation of the tunnel in TGS mode. Again, the harmonic case results in different behaviour to all of the other cases. The above investigation would suggest that a vehicle developed in an unsteady environment would essentially lead to the same order of magnitude in aerodynamic coefficients as developed in a conventional steady environment.

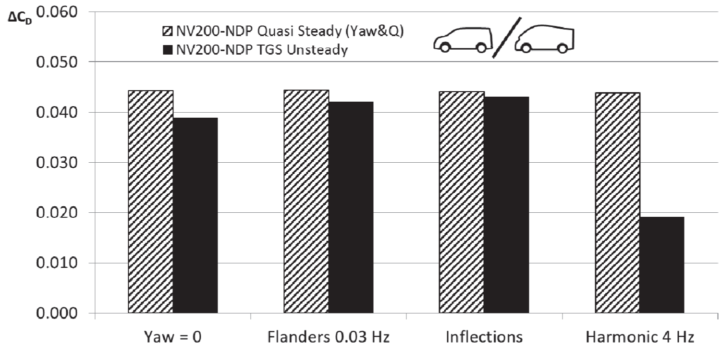

Figure 10. Variation of C_D between NV200 and NDP for steady and unsteady conditions.

4.5 Impact of Test Environment on Design Decisions

The variations of aerodynamic coefficients between two models for steady and unsteady conditions were described in the previous section. In this section smaller configuration changes are discussed and the question will be investigated whether different unsteady modes yield different results during configuration changes. The NDP base model was changed with add-on parts as illustrated in figure 11. These add-on aero parts are common in vehicle development programs and hence were chosen for this study. They comprise of front tyre deflectors, door mirrors, rear spoiler and rear side strakes.

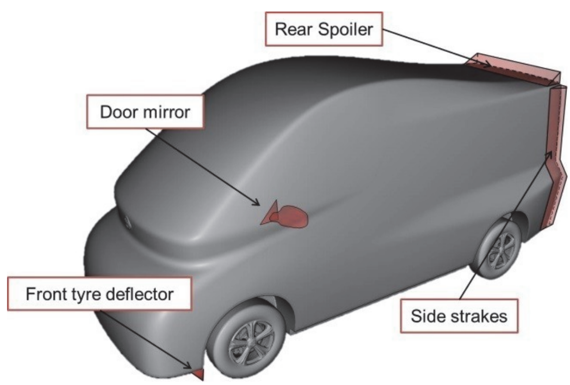

Figure 11. Illustration of the configuration changes on the NDP model.

The corresponding changes in C_D under steady and unsteady flow conditions are shown in figure 12. The changes in drag coefficient for the steady configuration were as expected; the front tyre deflectors reduced drag by 6 counts whereas the side strakes (12 counts), door mirrors (16 counts) and the rear spoiler (56 counts) caused an increase in drag. In the unsteady Inflections environment the trend was the same but the front tyre deflectors reduced drag by 11 counts, whereas the side strakes (7 counts), door mirrors (7 counts) and rear spoiler (41 counts) increased drag. Basically, the results mean the following: compared against the steady mode, in the unsteady environment the front tyre deflectors are more effective whilst the drag penalty with door mirrors, side strakes and rear spoiler is reduced. The Flanders unsteady mode showed comparable results to the Inflections mode. At this stage of the investigation no comparison of the tunnel boundary layer with regards to the effectiveness of the front tyre deflectors under steady and TGS mode was conducted.

All add-on aero parts showed the same ranking in steady and unsteady modes, except for the harmonic 4 Hz unsteady mode. All configurations resulted in a drag increase; front tyre deflector by 11 counts, side strakes by 29 counts, door mirror by 6 counts and the rear spoiler by 57 counts. The changes for the door mirror and rear spoiler showed good agreement with the steady mode.

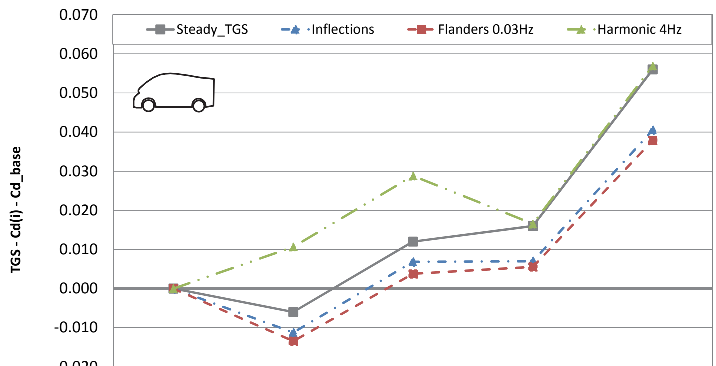

	NDP base	NDP FR tyre DEF	NDP Side Strakes	NDP Door Mirrors	NDP Rr. Spoiler
Steady_TGS	0.000	-0.006	0.012	0.016	0.056
Inflections	0.000	-0.011	0.007	0.007	0.041
Flanders 0.03Hz	0.000	-0.013	0.004	0.006	0.038
Harmonic 4Hz	0.000	0.011	0.029	0.017	0.057

Figure 12. Variation of C_d with add-on parts on the NDP.

Figure 13 shows the variation of the lift coefficient with the add-on parts between steady and unsteady modes. In the steady mode the front tyre deflector does not change C_{Ll}, the side strakes reduce lift by 7 counts whereas the door mirrors reduce lift by 15 counts. As expected, the rear spoiler configuration generates a substantial lift reduction of 104 counts. The variation in lift coefficient with the Inflections and Flanders unsteady modes are very similar to each other. In contrast to the steady mode, lift is increased with the front tyre deflector, side strakes and door mirrors. The rear spoiler results in less lift reduction in the unsteady mode compared to the steady mode.

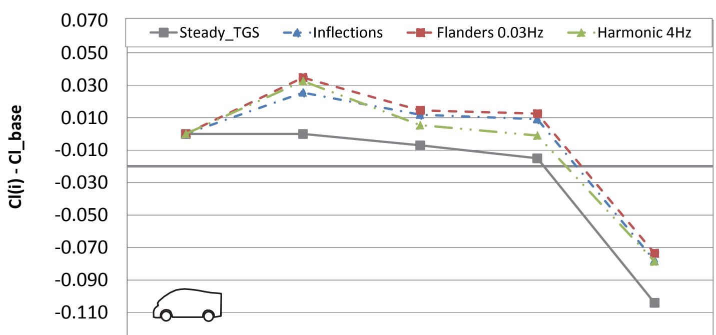

	NDP base	NDP FR tyre DEF	NDP Side Strakes	NDP Door Mirrors	NDP Rr. Spoiler
Steady_TGS	0.000	0.000	-0.007	-0.015	-0.104
Inflections	0.000	0.025	0.012	0.009	-0.078
Flanders 0.03Hz	0.000	0.035	0.015	0.012	-0.073
Harmonic 4Hz	0.000	0.033	0.005	-0.001	-0.078

Figure 13. Variation of lift coefficient for add-on parts on the NDP model for steady and unsteady conditions.

If we consider the above results as part of a vehicle development program and neglecting eventual interaction effects, then the steady mode would indicate a total drag increase of 78 counts whereas the Inflections and Flanders unsteady modes would indicate an increase of 43 and 34 counts respectively. In addition, the variation in total lift coefficient between steady and unsteady modes, especially for the rear spoiler configuration, varies between -126 counts for the steady and -32 and -12 counts for the Inflections and Flanders mode respectively. In other words, the final shape of the vehicle selected could be different depending on the flow conditions or wind tunnel simulation mode used during a vehicle development program.

5 CONCLUSIONS

Geometries representing early and late stages of a vehicle development program have been investigated under several steady and unsteady flow conditions to better understand the impact of the chosen test conditions on absolute drag, on drag differences between distinct vehicles, and on smaller scale design decisions.

Flows including non-zero yaw would be expected to lead to an increase in the time-averaged drag coefficient. However, in this work drag increments under unsteady flow conditions were generally less than would be predicted by a quasi-steady analysis and in some cases unsteadiness led to a drag reduction. These differences between quasi-steady and time-averaged unsteady drag were found to be linked to base pressures.

The drag difference for different vehicle shapes was found to be slightly lower but in the same order of magnitude for unsteady modes to that measured at zero yaw under conventional test conditions. However, the impact of small configuration changes was found to be different in an unsteady environment to a zero yaw condition, in terms of both drag and lift. Therefore, design decisions could be different according to whether the vehicle is optimised under steady zero yaw conditions or subject to a representative unsteady flow.

6 ACKNOWLEDGEMENTS

The authors are grateful to Nissan Technical Centre Europe for permission to publish this paper and to Innovate UK for funding this project. Special thanks go to Bob Bateman, Peter Barron and Kingsley Hanlon from NTCE as well as Darryl Scriven and Dean Claridge from NDE for their enthusiasm and support for the development programme. Thanks are also offered to the team at CGI for the CAD support and model manufacturing solutions, as well as Paul Dancer and Louise Lam from Cranfield University for the instrumentation of the scale model. Additional thanks to Zitong Zhang for the valuable discussions on post-processing.

REFERENCE LIST

(1) Kremheller, A., "The Aerodynamics Development of the New Nissan Qashqai," SAE Technical Paper 2014-01- 0572, 2014, doi:10.4271/2014-01-0572.
(2) Howell, J., "Aerodynamic Drag in a Windy Environment," IMechE International Vehicle Aerodynamics Conference, Loughborough University, 2014.
(3) Howell, J., "Aerodynamic Drag of Passenger Cars at Yaw," SAE Int. J. Passeng. Cars - Mech. Syst. 8(1):2015, doi:10.4271/2015-01-1559.

(4) Windsor, S., "Real World Drag Coefficient – Is it Wind Averaged Drag?," IMechE International Vehicle Aerodynamics Conference, Loughborough University, 2014.
(5) Gaylard, A., Oettle, N., Gargoloff, J., and Duncan, B., "Evaluation of Non-Uniform Upstream Flow Effects on Vehicle Aerodynamics," SAE Int. J. Passeng. Cars - Mech. Syst. 7(2):2014, doi:10.4271/2014-01-0614.
(6) D'Hooge, A., Palin, R., Rebbeck, L., Gargoloff, J. et al., "Alternative Simulation Methods for Assessing Aerodynamic Drag in Realistic Crosswind," SAE Int. J. Passeng. Cars - Mech. Syst. 7(2):617-625, 2014, doi:10.4271/2014-01-0599.
(7) Wordley, S., and Saunders, J., "On-Road Turbulence", SAE Technical Paper Series, 2008-01-0475, 2008.
(8) Sims-Williams, D., "Cross Winds and Transients: Reality, Simulation and Effects," SAE Int. J. Passeng. Cars - Mech. Syst. 4(1): 172-183, 2011, doi:10.4271/2011-01-0172.
(9) Mankowski, O., Sims-Williams, D., and Dominy, R., "A Wind Tunnel Simulation Facility for On-Road Transients," SAE Int. J. Passeng. Cars - Mech. Syst. 7(3):2014, doi:10.4271/2014-01-0587.
(10) Stoll, D., Kuthada, T., Wiedemann, J., and Schütz, T., "Unsteady Aerodynamic Vehicle Properties of the DrivAer Model in the IVK Model Scale Wind Tunnel.," 10th FKFS Progress in Vehicle Aerodynamics and Thermal Management, 2015.
(11) Kremheller, A., Le Good, G., Annetts, I., and Moore, M., "The Aerodynamics Development of a New Light Commercial Vehicle Concept Under Uniform and Transient Flow Conditions.," 10th FKFS Progress in Vehicle Aerodynamics and Thermal Management, 2015.
(12) Sims-Williams, D and Dominy, R. The Design of a New Wind Tunnel for Vehicle Aerodynamics Research, MIRA Vehicle Aerodynamics Conference. Warwick, UK, 2002.
(13) Sims-Williams, D and Dominy, R. The Design of an Open-Jet Wind Tunnel for Model Testing, SAE Paper 2002-01-3340. SAE Motorsports Engineering Conference. Indianapolis, 2002.
(14) Oettle, N., Sims-Williams, D., and Dominy, R., "Assessing the Aeroacoustic Response of a Vehicle to Transient Flow Conditions from the Perspective of a Vehicle Occupant," SAE Int. J. Passeng. Cars - Mech. Syst. 7(2):550-558, 2014, doi:10.4271/2014-01-0591.
(15) Sims-Williams, DB, Dominy, RG, The Validation and Application of a 5 Hole Pressure Probe with Tubing Transfer Correction for Time-Accurate Measurements in Unsteady Flows, Second MIRA International Conference on Vehicle Aerodynamics, Coventry, 1998.
(16) Society of Automotive Engineers, Aerodynamic Testing of Road Vehicles in Open Jet Wind Tunnels, SP-1465, SAE, Warrendale, PA, 1999.
(17) Flanders, R. An Investigation of the Effect of Varying Yaw on Aerodynamic Drag, MEng Dissertation, Durham University, 2014.
(18) Mercker, E., and Wiedemann, J., "On the Correction of Interference Effects in Open Jet Wind Tunnels," SAE 960671.